APPENDIX A

Spectrofluorometric determination of intracellular levels of reactive oxygen species in drug-sensitive and drug-resistant cancer cells using the 2', 7'-dichlorofluorescein diacetate assay

Published in
Radiation Physics and Chemistry

Volume 72: 323–331 (2005)
doi:10.1016/j.radphyschem.2004.06.011

Available online at www.sciencedirect.com
SCIENCE DIRECT®
Radiation Physics and Chemistry 72 (2005) 323–331
Radiation Physics and Chemistry
www.elsevier.com/locate/radphyschem

Spectrofluorometric determination of intracellular levels of reactive oxygen species in drug-sensitive and drug-resistant cancer cells using the 2′,7′-dichlorofluorescein diacetate assay☆

Chatchanok Loetchutinat[a], Suchart Kothan[a], Samarn Dechsupa[a], Jintana Meesungnoen[a,b], Jean-Paul Jay-Gerin[b], Samlee Mankhetkorn[a,*]

[a]*Laboratory of Physical Chemistry, Molecular and Cellular Biology, Faculty of Science, Burapha University, Bangsaen, Chonburi 20131, Thailand*
[b]*Département de médecine nucléaire et de radiobiologie, Faculté de médecine, Groupe en sciences des radiations, Université de Sherbrooke, Sherbrooke, Québec, Canada J1H 5N4*

Received 16 February 2004; accepted 7 June 2004

Spectrofluorometric determination of intracellular levels of reactive oxygen species in drug-sensitive and drug-resistant cancer cells using the 2', 7'-dichlorofluorescein diacetate assay+

Chatchanok Loetchutinat[a], Suchart Kothan[a], Samarn Dechsupa[a], Jintana Meesungneon[a,b], Jean-Paul Jay-Gerin[b], Samlee Mankhetkorn[a,*]

[a] *Laboratory of Physical Chemistry, Molecular and Cellular Biology, Faculty of Science, Burapha University, Bangsaen, Chonburi 20131, Thailand*

[b] *Groupe en sciences des radiations, Département de médecine nucléaire et de radiobiologie, Faculté de médecine, Université de Sherbrooke, Sherbrooke (Québec) J1H 5N4, Canada*

+ This paper is dedicated to the memory of Professor Christiane Ferradini, in gratitude for all she gave us.

Abstract

This article examines a non-invasive spectrofluorometric method using the 2', 7'-dichlorofluorescein diacetate (DCHF-DA) assay for quantifying the intracellular reactive oxygen species (ROS_i) produced in four cultured cancer cell lines: drug-sensitive (K562) and drug-resistant (K562/*adr*) human erythromyelogenous leukemia cell lines, and drug-sensitive (GLC4) and drug-resistant (GLC4/*adr*) human small cell lung carcinoma cell lines. The oxidation of the probe to the fluorescent dichlorofluorescein (DCF) was continuously monitored by following the DCF fluorescence intensity as a function of time using a standard spectrofluorometer in the presence of an extracellular DCF fluorescence quencher (Co^{2+}). By fitting the spectrofluorometric data to a kinetic model based on the following two reactions: (i) deacetylation of DCHF-DA to the oxidant-sensitive compound 2′, 7′-dichlorofluorescein (DCHF) by cellular esterase enzymes (pseudo-first-order rate constant: k_e) and (ii) oxidation of DCHF by ROS_i (second-order rate constant: k_2), the parameters intervening in the DCF formation, k_e and the product of k_2 by the ROS_i concentration, were quantitatively determined for the different cell lines studied. The results revealed that the intracellular esterase content or activity is similar in K562, K562/*adr*, and GLC4 cells, but 5-fold higher in GLC4/*adr* cells. The product $k_2[ROS_i]$ was found to be similar in the four cell lines considered, with a mean value of $(5.3 \pm 0.9) \times 10^{-7}$ $cell^{-1}$ s^{-1}. Assuming that H_2O_2 (in combination with peroxidases) is the primary responsible species for DCHF oxidation in intact cells, and using the rate constant value $k_2 = 790 \pm 62$ M^{-1} s^{-1} established in our laboratory for the reaction of DCHF with H_2O_2 in the presence of horseradish peroxidase, the mean value of the intracellular levels of ROS_i in those cells was estimated to be 0.67 ± 0.16 nM per cell. Such a value compares favorably to H_2O_2 intracellular steady-state concentrations that have been estimated in the literature for a few other cell types.

Keywords: 2′,7′-dichlorofluorescein diacetate (DCHF-DA); Multidrug resistance (MDR); Intracellular reactive oxygen species (ROS_i); Physiological ROS_i concentrations; Oxidative stress; Spectrofluorometry

***Corresponding author**: *Tel.: (66) 38-745900, ext. 3098; Fax: (66) 38-745199*
E-mail address: samlee@bucc4.buu.ac.th

INTRODUCTION

Free radicals are important intermediates constantly produced in vivo through a variety of normal metabolic processes as well as being common intermediates generated after exposure to drugs, xenobiotics or ionizing radiation (Curtin *et al.*, 2002). The last decade has seen a huge surge of interest in free radicals in biology, and the pathogenesis of many diseases has been associated with reactive oxygen species (ROS) (Halliwell and Gutteridge, 1999). Furthermore, the uncontrolled generation of ROS may lead to aging, inflammation, and neurodegenerative disorders (Sun and Chen, 1998). Although free radicals are usually considered to cause oxidative damage to the living organism, some of these such as nitric oxide ($^{\bullet}NO$) and the superoxide radical ($O_2^{\bullet-}$) also have beneficial functions including, for example, the regulation of blood pressure and blood flow (Viidas *et al.*, 1998), the induction of macrophage tumor cytotoxicity (Cui *et al.*, 1994), and the phagocytic killing of harmful bacteria (Rosen *et al.* 1995). In order to determine the diverse roles of ROS in biological systems, many research groups performed their works focusing on the effects of endogenous and exogenous ROS in a variety of cell types, using 2′,7′-dichlorofluorescein diacetate (DCHF-DA) as a sensitive, cell permeable probe for the detection of intracellular ROS (ROS_i) (Keston and Brandt, 1965; Brandt and Keston, 1965). It has been demonstrated that the lipophilic, nonfluorescent DCHF-DA can readily cross cell membranes by passive diffusion and undergoes deacetylation by intracellular esterase enzymes, producing the non-fluorescent, oxidant-sensitive 2′, 7′-dichlorofluorescein (DCHF), which is trapped inside the cells. In the presence of hydrogen peroxide (H_2O_2) and other ROS as well as heme protein catalysts, such as peroxidases or cytochrome *c*, DCHF is oxidized to highly fluorescent 2′, 7′-dichloro-fluorescein (DCF) (LeBel *et al.*, 1992; Ischiropoulos *et al.*, 1999; Burkitt and Wardman, 2001; Ohashi *et al.*, 2002). The DCF fluorescence intensity can be easily measured and is the basis of the cellular assay for detecting intracellular levels of ROS. The DCHF-DA assay has commonly been performed in association with the techniques of flow cytometry (Bass *et al.*, 1983; Amer *et al.*, 2003), microfluoro-metry (Wan *et al.*, 1993), fluoro-imaging analysis (Minamiya *et al.*, 1995), microscopy (Aoyagi *et al.*, 1999), and confocal scanning laser microscopy (Sheng *et al.*, 2002). Although there is clear evidence that DCHF-DA is able to directly assess the redox state in most cell systems, it must be pointed out, however, that some limitations of using this probe exist. DCF, the oxidized fluorescent product of DCHF, is membrane permeable and can leak out of cells over time (Ubezio and Civoli, 1994). Incomplete DCF trapping may complicate interpretation of the data and hinder the precise evaluation of intracellular oxidation. In addition, some cell types have low esterase activity. This may limit the availability of DCHF and result in an underestimation of ROS_i levels (Brubacher and Bols, 2001). Moreover, it remains unclear which oxidative species is responsible for the oxidation of DCHF in cells, even though it is often assumed to be H_2O_2 (in combination with cellular peroxidases and similar catalysts). There was reported that other biologically

relevant ROS, including peroxynitrite ($ONOO^-$) and hydroxyl radicals ($^{\bullet}OH$), can oxidize DCHF (Myhre *et al.*, 2003). Up to date, the DCHF-DA assay has been extensively used to measure the levels of oxidative stress and ROS generation in many cell types in response to a variety of stimuli or environmental stresses. However, measurements of physiological ROS_i concentrations in intact cells are scarce due to the dearth of appropriate experimental methods.

In the present work, the DCHF-DA assay was used in conjunction with conventional spectrofluorometry in an attempt to quantify basal levels of ROS_i in various cancer cell lines. In brief, the oxidation of the probe to the fluorescent DCF was continuously monitored by following the DCF fluorescence intensity using a standard spectrofluorometer in the presence of cells and an extracellular DCF fluorescence quencher (Co^{2+}). By model fitting the spectrofluorometric data, the parameters intervening in the DCF formation, namely, the rate constant of the esterase-catalyzed conversion of DCHF-DA to DCHF and the product of the rate constant of DCHF oxidation by the ROS_i concentration, were quantitatively determined in both drug-sensitive (K562 and GLC4) and drug-resistant (K562/*adr* and GLC4/*adr*) cell lines. Assuming that H_2O_2 (in the presence of a catalyst) is the oxidant species that offers the greater ability to oxidize DCHF in intact cells, ROS_i concentrations were then estimated by using a value of k_2 established in our laboratory for the reaction of DCHF with H_2O_2 in the presence of horseradish peroxidase.

A preliminary report of this work has been presented elsewhere (Loetchutinat *et al.*, 2003).

MATERIALS AND METHODS

Drugs and chemicals

2′, 7′-Dichlorofluorescein diacetate (DCHF-DA) was purchased from Molecular Probes, Inc. (Eugene, OR, USA). Tetrazolium salt, 3-(4, 5-dimethyl-2-thiazolyl)-2, 5-diphenyl-2*H*-tetrazolium bromide (MTT), trypan blue, saponin, and $CoCl_2$ were obtained from Sigma Chemical Co. (St. Louis, MO, USA). Doxorubicin (DOX) and pirarubicin (THP) were from Laboratoire Roger Bellon (Neuilly-sur-Seine, France) and kindly provided by Professor Arlette Garnier-Suillerot (Laboratoire de Physico-chimie Biomoléculaire et Cellulaire, Université Paris Nord, Bobigny, France).

DOX and THP stock solutions were freshly prepared in deionized double-distilled water just before use. Concentrations were spectrophotometrically determined by diluting stock solutions in water to ~10 μM and using a molar extinction coefficient ε_{480nm} = 11,500 $M^{-1}cm^{-1}$ for both anthracycline molecules (Mankhetkorn *et al.*, 1996). A stock solution of MTT was prepared by dissolving 5 mg MTT/mL in HEPES-Na^+ buffer and then filtering through a 0.22-μm filter, and was stored at 4 °C.

All experiments were performed using HEPES-Na^+ buffer solutions consisting of 20 mM HEPES buffer plus 132 mM NaCl, 3.5 mM KCl, 1 mM $CaCl_2$, and 1.5 mM $MgCl_2$ (pH 7.25 at 37 °C).

Cell culture and cytotoxicity assay

The K562 human erythromyelogenous leukemia cell line and its DOX-resistant, P-glycoprotein-overexpressing K562/*adr* subline (Tarasiuk *et al.*, 1993; Mankhetkorn *et al.*, 1996), and the GLC4 human small cell lung carcinoma cell line and its DOX-resistant, MRP1-overexpressing GLC4/*adr* subline (Reungpatthanaphong *et al.*, 2003) were used in this study. Cells were routinely cultured in RPMI 1640 medium supplemented with 10% (v/v) fetal calf serum (Gibco Biocult Ltd., Paisley, Scotland) in a humidified atmosphere of 95% air and 5% CO_2 at 37 °C. For the assays, cell cultures were initiated at a density of 5×10^5 cells/mL to have cells in the exponential growth phase; the cells were used 24 h later when the culture had grown to about 8×10^5 cells/mL. Cell viability was assessed by trypan blue exclusion. The number of cells was determined with a haemocytometer.

The cytotoxicity assay was performed as follows. Cells (5×10^4 cells/mL) were incubated in the presence of various THP concentrations. The viability of cells was then determined using the MTT assay based on the reduction of MTT to purple-colored formazan by live, but not dead, cells. The concentration of THP required to inhibit cell growth by 50% when measured at 72 h (IC_{50}) was determined by plotting the percentage of cell growth inhibition versus the pirarubicin concentration. The resistance factor (RF) was defined as the IC_{50} of resistant cells divided by the IC_{50} of the corresponding sensitive cells (Mankhetkorn *et al.*, 1996). Under our experimental conditions, the IC_{50} values were 10 ± 2 nM for K562 and GLC4 cells. The RF values were 40 and 7 for K562/*adr* and GLC4/*adr* cells, respectively.

Physicochemical properties of DCHF-DA

In aqueous solution, DCHF-DA and DCF were shown to possess an absorption maximum at 320 and 502 nm, respectively. In basic solution (pH > 8), the absorbance at 502 nm increased steeply with increasing pH, due to the rapid hydrolysis of DCHF-DA to DCHF and to the final product DCF. A plateau was then attained at pH 11, signifying that DCHF-DA was totally converted to DCF (Fig. 1). The purity of DCF was verified by thin layer chromatography (data not shown). Known concentrations of DCF were prepared from the diacetate by alkaline hydrolysis in aqueous solutions whose pH was adjusted to 13 using 5*N* NaOH. A 1:1 stoichiometry was observed with 1 mole of DCF produced per mole of DCHF-DA.

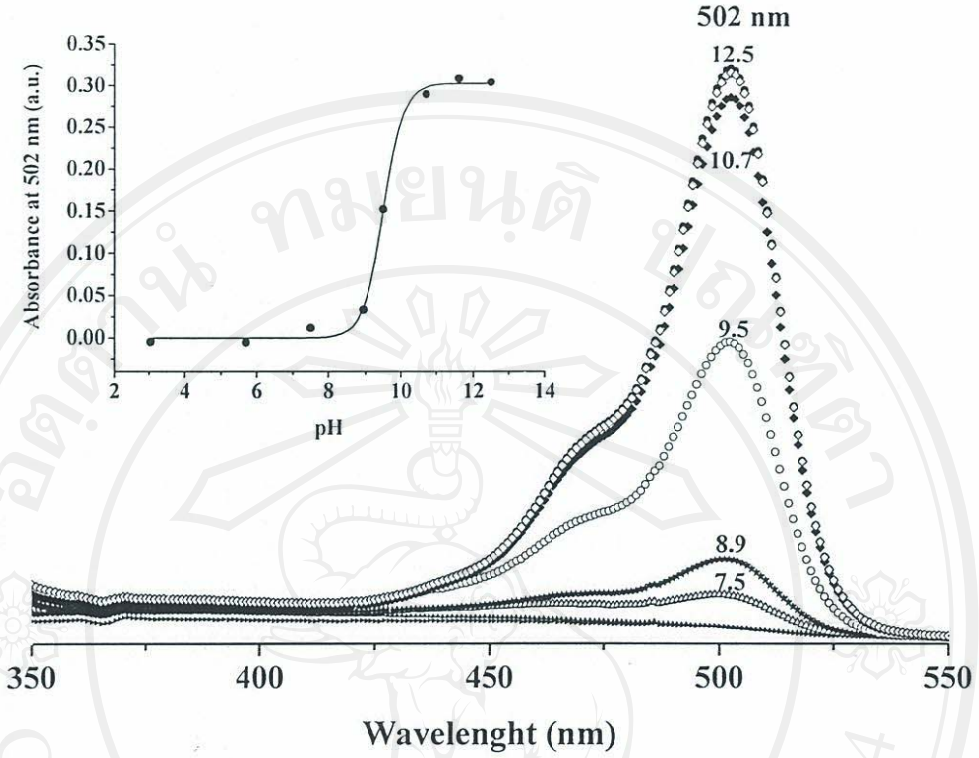

Figure 1. Absorption spectra of DCHF-DA in aqueous solution with the indicated pH. Inset: variation of the absorbance at 502 nm as a function of pH.

Determination of the intracellular DCF concentration

Considering the cell culture system, some amounts of ROS, notably H_2O_2, were detected in the extracellular environment or in the medium (Grzelak *et al.*, 2001; Halliwell, 2003). In order to localize the interaction of ROS_i and DCHF that occurs inside of cells only, use was made of the extracellular DCF fluorescence quencher Co^{2+} (Homan and Eisenberg, 1985; Morris *et al.*, 1985). In the presence of 20 mM Co^{2+}, an increase in fluorescence intensity was due to an increase in DCF formation inside the cells. Details of the use of Co^{2+} as an efficient quencher of extracellular DCF fluorescence are given in the results section.

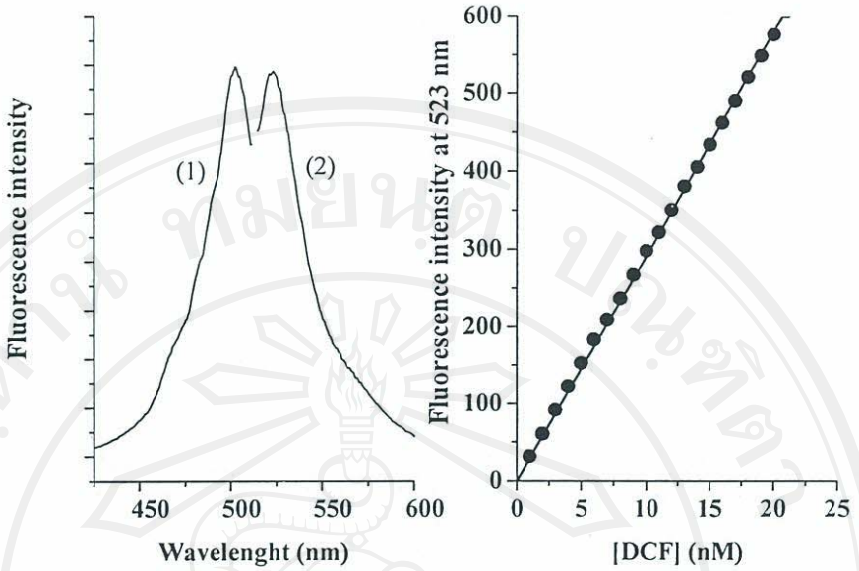

Figure 2. (a) Excitation (1) and emission (2) spectra of DCF in HEPES-Na^+ buffer. (b) DCF fluorescence intensity at 523 nm (excitation at 502 nm) versus concentration of DCF. This linear relationship allows conversion of the fluorescence data to units of DCF concentration. The concentration of DCF (in nanomolar) in the experimental sample is obtained by dividing the measured DCF fluorescence intensity by 31.6.

DCF has an emission spectrum with a maximal intensity at 523 nm when excited at 502 nm (Fig. 2a), but not DCHF-DA nor DCHF, which provides a very good advantage for monitoring the final product of deacetylation and oxidation of DCHF-DA in the solution without any purification. The fluorescence intensity at 523 nm was proportional to the concentration of DCF at least in the range of DCF concentrations used in this study (Fig. 2b). Fluorescence values were converted to DCF concentrations by reference to this linear relationship. The fluorescence intensity per molar of DCF at 523 nm (with 502 nm excitation) was equal to 31.6×10^9 M^{-1}.

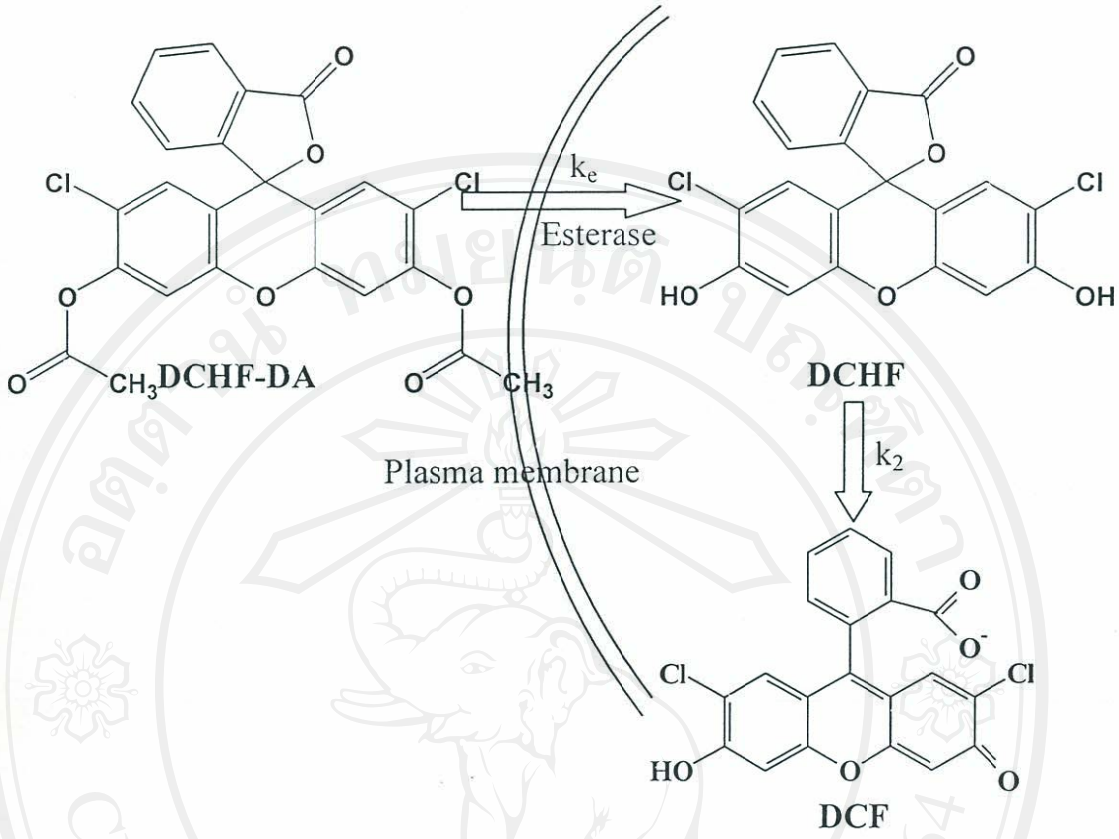

Figure 3. Mechanism of action of 2',7'-dichlorofluorescein diacetate (DCHF-DA).

Theoretical approach

In a first approximation, the uptake of DCHF-DA into cells and the subsequently observed DCF fluorescence intensity are assumed to proceed via the following mechanism (Fig. 3): (i) DCHF-DA is readily taken up by cells via passive diffusion across the plasma membrane, (ii) DCHF-DA is deacetylized by cellular esterase enzymes to yield the oxidant-sensitive DCHF, and (iii) DCHF oxidation by ROS_i generates the highly fluorescent DCF. The overall scheme can be modeled by the consecutive reactions (1) and (2):

$$\text{DCHF–DA} \xrightarrow[\text{slow}]{\text{esterase},\ k_1} \text{DCHF} \qquad (1)$$

$$\text{DCHF} + \text{ROS}_i \xrightarrow[\text{fast}]{k_2} \text{DCF} \qquad (2)$$

The nature of reaction (2) that involves reactive oxygen species leads us to hypothesize that the formation of the intermediate DCHF, which results from the enzyme-catalyzed reaction of DCHF-DA, is slower than its consumption (in other words, the reaction step (1) is the rate determining step in the mechanism). Assuming reaction (1) to be pseudo first order, that is, no depletion of intracellular esterase levels is considered over the time course of the experiments, the rate of DCHF-DA disappearance (or DCHF production) is given by:

$$\frac{d[\mathrm{DCHF-DA}]}{dt} = -k_1[\mathrm{E}]_0[\mathrm{DCHF-DA}] \tag{3}$$

from which we get, upon integration,

$$[\mathrm{DCHF-DA}] = [\mathrm{DCHF-DA}]_0\, e^{-k_1[\mathrm{E}]_0 t}, \tag{4}$$

where $[\mathrm{E}]_0$ is the intracellular esterase concentration and $[\mathrm{DCHF\text{-}DA}]_0$ is the initial concentration of DCHF-DA inside the cells. Note the simplification made here that the rapid uptake of DCHF-DA into cells is approximated by a step function in the DCHF-DA concentration in the cells, which varies from 0 to $[\mathrm{DCHF\text{-}DA}]_0$ at $t = 0$. As for DCHF, the rate equation is:

$$\frac{d[\mathrm{DCHF}]}{dt} = k_1[\mathrm{E}]_0[\mathrm{DCHF-DA}] - k_2[\mathrm{ROS_i}][\mathrm{DCHF}] \tag{5}$$

Integration of Eq. (5) gives:

$$[\mathrm{DCHF}] = \frac{k_1[\mathrm{E}]_0\,[\mathrm{DCHF-DA}]_0}{k_2[\mathrm{ROS_i}] - k_1[\mathrm{E}]_0}\left(e^{-k_1[\mathrm{E}]_0 t} - e^{-k_2[\mathrm{ROS_i}]t}\right) \tag{6}$$

The rate of appearance of DCF can be written as:

$$\frac{d[\mathrm{DCF}]}{dt} = k_2[\mathrm{DCHF}][\mathrm{ROS_i}]$$

Replacing [DCHF] by its expression of Eq. (6) and integrating, Eq. (7) gives:

$$[\mathrm{DCF}] = \frac{[\mathrm{DCHF-DA}]_0}{k_2[\mathrm{ROS_i}] - k_e}\left(k_2[\mathrm{ROS_i}](1 - e^{-k_e t}) - k_e(1 - e^{-k_2[\mathrm{ROS_i}]t})\right) \tag{8}$$

where $k_e = k_1[\mathrm{E}]_0$ is the pseudo-first-order rate constant for reaction (1) (in s^{-1}).

The model is mathematically expressed in Eq. (8) and the parameters intervening in the DCF formation, k_e and $k_2[\mathrm{ROS_i}]$, can be quantitatively determined by fitting Eq. (8) to the experimental spectrofluorometric data.

Some caution should, however, be exercised here; in fact, Eq. (8) does not a priori allow an unambiguous determination of the two rate constants since it can be seen that they are perfectly symmetrical. Fortunately, this so-called slow-fast ambiguity (for example, see: Gutfreund, 1995) can easily be removed in the problem at hand taking into account that the consumption rate of the intermediate DCHF is faster than its formation rate. Under such conditions, the correct choice of constants to be made in the fitting process of Eq. (8) to the data must then necessarily correspond to $k_2[ROS_i]$ larger than k_e.

The series of experiments to quantify ROS_i using DCHF-DA were performed in the four cancer cell lines K562, K562/*adr*, GLC4, and GLC4/*adr*. The fluorescence of the cells was monitored as a function of time on a Perkin-Elmer LS-50B spectrofluorometer with excitation and emission wavelengths of 502 and 523 nm, respectively.

RESULTS AND DISCUSSION

Figure 4a shows representative results of DCHF-DA oxidation by ROS_i in intact cells. Drug-sensitive and drug-resistant cells (10^5 cells/mL) were suspended in a 1-cm quartz cuvette containing 2mL of HEPES-Na^+ buffer (pH 7.25) at 37 °C under vigorous stirring during 10 min, followed successively by the addition of 20 mM $CoCl_2$ (extracellular DCF fluorescence quencher) and 100 nM DCHF-DA. As mentioned above, under those experimental conditions, the increase in DCF fluorescence intensity at 523 nm should correspond only to the intracellular not the extracellular DCF. To confirm our hypothesis, the kinetics of DCF appearance in the presence of Co^{2+} is significantly slower than that of the experiments carried out without the addition of cobalt. In addition, experiments were also performed in the sole presence of 20 mM $CoCl_2$ and 100 nM DCHF-DA in buffer without cells; no DCF fluorescence was detected. This signifies that the DCF fluorescence intensity in the series of experiments with Co^{2+} reflects only the interaction of DCHF-DA and intracellular ROS. Indeed, the DCF fluorescence intensity at 523 nm is observed to steeply decrease with increasing concentration of $CoCl_2$; ~80% DCF fluorescence extinction was obtained when using 20 mM $CoCl_2$ (Fig. 4b).

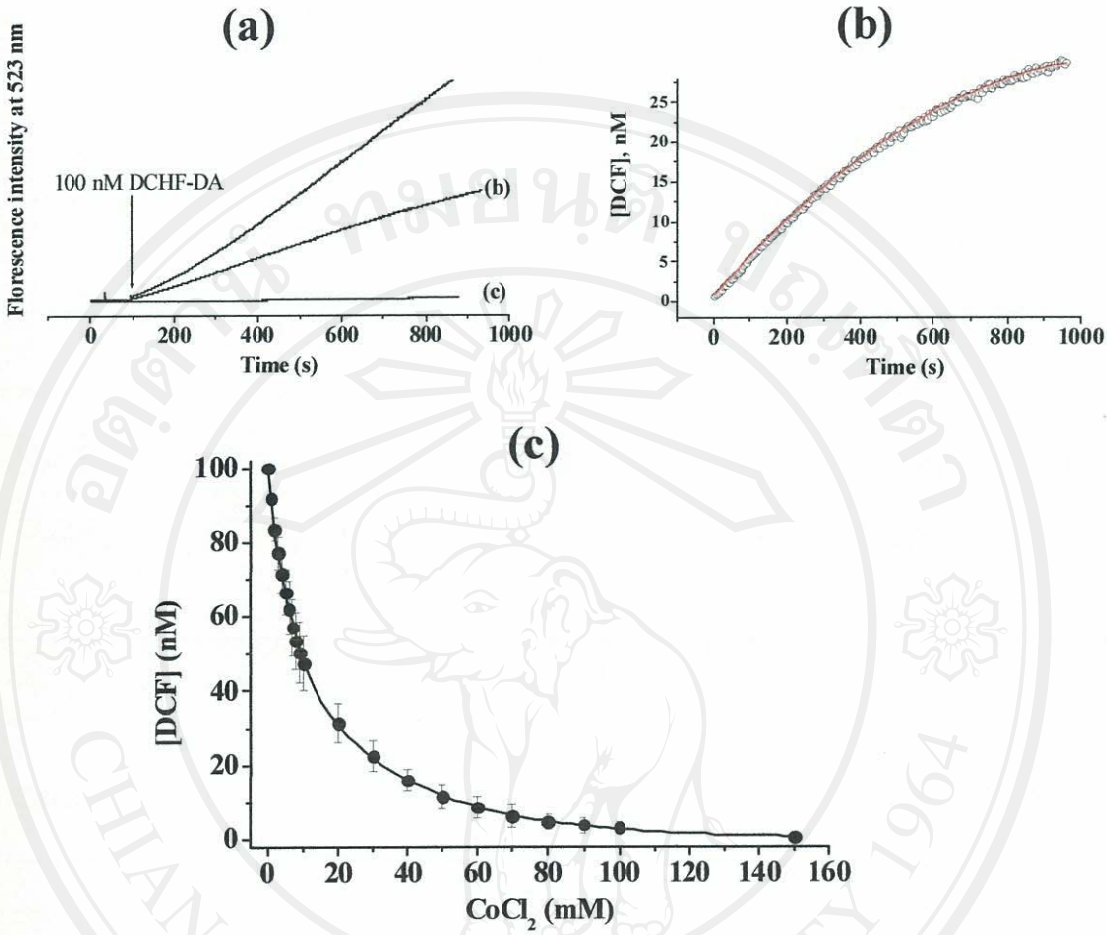

Figure 4. (a) Kinetics of DHCF-DA oxidation: K562 cells (2×10^5) were suspended in 2 mL of HEPES-Na^+ buffer for 10 min before addition of either 100 nM DCHF-DA (i) or 20 mM $CoCl_2$ and 100 nM DCHF-DA (ii). Trace (iii) corresponds to the addition of 20 mM $CoCl_2$ and 100 nM DCHF-DA but without cells. The DCF fluorescence intensity at 523 nm (excitation at 502 nm) was recorded as a function of time. (b) The effect of Co^{2+} as a quencher for DCF fluorescence intensity. (c) The DCF fluorescence intensity obtained from the series of experiments (ii) was converted to DCF concentration as a function of time. The origin of time corresponds here to the time at which 100 nM DCHF-DA were added to the medium (○, experimental data; ——, fitted curve computed using Eq. (8)).

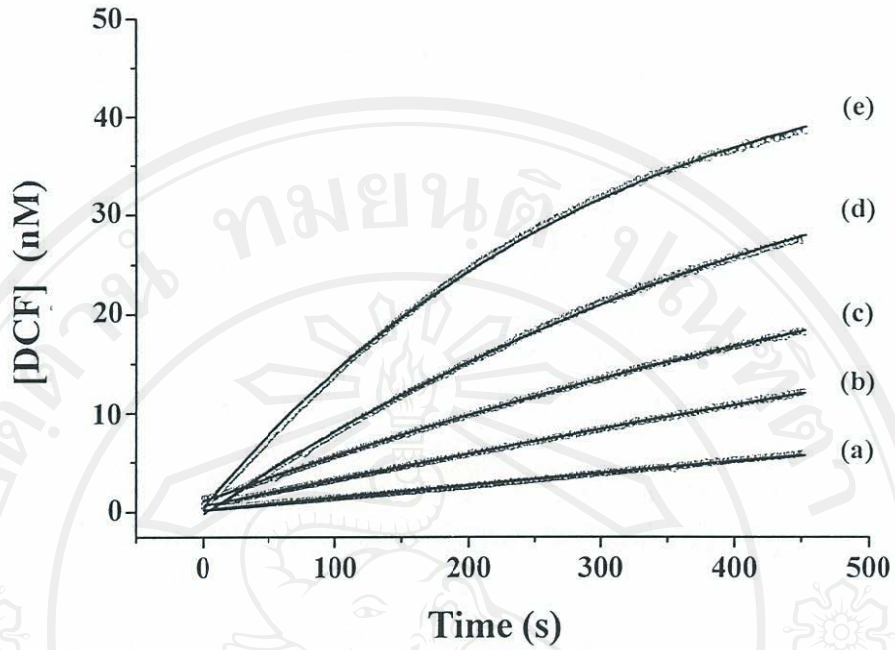

Figure 5. Kinetics of DCHF-DA oxidation performed for different concentrations of K562 cells: (a) 0.5×10^5, (b) 1×10^5, (c) 2×10^5, (d) 4×10^5, and (e) 6×10^5 cells were suspended in 2 mL of HEPES-Na^+ buffer for 10 min before addition of 20 mM $CoCl_2$ and 100 nM DCHF-DA. The DCF fluorescence intensity at 523 nm (excitation at 502 nm) was recorded and converted to DCF concentration as a function of time. The origin of time corresponds to the time at which DCHF-DA was added to the medium (○, experimental data; ——, fitted curve computed using Eq. (8)).

The concentration of DCF as a function of time was modeled by Eq. (8) and the kinetic parameters k_e and $k_2[ROS_i]$ were derived by fitting this equation to the experimental data obtained for different concentrations of the four cell lines studied (Figs. 4c and 5). The use of Eq. (8), which relies on the assumption of a complete DCF trapping within cells, is justified here since in our experimental conditions no leakage of DCF out of cells was observed over time for both drug-sensitive and drug-resistant cell lines. Table 1 lists the results of the analysis. As can be seen, the mean pseudo-first-order rate constant ($k_e = k_1[E]_0$) of reaction (1) is similar in K562, K562/*adr*, and GLC4 cells, equal to $(6.5 \pm 1.3) \times 10^{-9}$ $cell^{-1}$ s^{-1}, but 5-fold higher in GLC4/*adr* cells. These results suggest that the intracellular esterase contents in GLC4/*adr* cells should be higher or more active than those in K562, K562/*adr* and GLC4 cells. As for reaction (2), the product $k_2[ROS_i]$ is found to be similar in the four cell lines considered, with a mean value of $(5.3 \pm 0.9) \times 10^{-7}$ $cell^{-1}$ s^{-1}. For the very low DCHF-DA concentration (such as 100 nM) used in our experiments, the determination of

$[ROS_i]$ depends directly on k_2, but not on the DCHF concentration or the esterase activity. The choice of k_2 which should be used to determine $[ROS_i]$ is obviously most sensitive since various intracellular oxidant species, including H_2O_2 (in combination with cellular peroxidases), $ONOO^-$, and $^{\bullet}OH$ radicals (Myhre *et al.*, 2003), were demonstrated to react with DCHF. Note that we have also previously observed that DCHF undergoes reaction with hydroxyl radicals (data not shown). According to Myhre *et al.* (2003), DCHF shows only a low sensitivity toward oxidation by $^{\bullet}NO$, HOCl (hypochlorous acid), and $O_2^{\bullet-}$ in cellular systems. In intact cells, which is the case of interest here, H_2O_2 (in the presence of a catalyst) is likely to be the species that offers the greater ability to react with DCHF. In fact, under normal physiological conditions, the relatively low levels of $^{\bullet}NO$ (~1-10 nM) produced by constitutive nitric oxide synthases (cNOS) associated with the low intracellular concentrations of $O_2^{\bullet-}$ (~10-100 pM) (Halliwell and Gutteridge, 1999; Giulivi *et al.*, 1999; Cadenas and Davies, 2000) seem to preclude any significant role of peroxinitrite (which can form by the combination of $^{\bullet}NO$ and $O_2^{\bullet-}$). As for $^{\bullet}OH$ radicals, their reaction with DCHF is unlikely to occur because the steady-state concentration of $^{\bullet}OH$ is very small ($\sim 10^{-14}$ M), expressing the high reactivity (and small selectivity) of those species. In fact, it was suggested that the lifetime of an $^{\bullet}OH$ radical in a cell was a few nanoseconds and its diffusion distance therefore a few nanometers (Mikkelsen and Wardman, 2003). Huge concentrations of DCHF would therefore be needed to compete with biological molecules for any $^{\bullet}OH$ generated.

Table 1. Mean rate constant (k_e) of the DCHF-DA deacetylation catalyzed by intracellular esterases (pseudo-first-order reaction), the product $k_2[ROS_i]$, and the ROS_i levels per cell determined in K562, K562/*adr*, GLC4, and GLC4/*adr* cell lines ($1.5\text{-}2.0 \times 10^5$ cells), using $k_2 = 790 \pm 62\ M^{-1}\ s^{-1}$ for the second-order rate constant for the reaction of DCHF with H_2O_2 in the presence of horseradish peroxidase (see text).

Cell line	$k_e = k_1[E]_0$ (cell^{-1} s^{-1})	$k_2[ROS_i]$ (cell^{-1} s^{-1})	$[ROS_i]$ (nM cell^{-1})
K562	$(6.1 \pm 0.5) \times 10^{-9}$	$(5.2 \pm 0.3) \times 10^{-7}$	0.66 ± 0.09
K562/*adr*	$(7.3 \pm 3.1) \times 10^{-9}$	$(4.7 \pm 1.1) \times 10^{-7}$	0.59 ± 0.19
GLC4	$(6.0 \pm 0.2) \times 10^{-9}$	$(5.1 \pm 1.3) \times 10^{-7}$	0.65 ± 0.22
GLC4/*adr*	$(31 \pm 13) \times 10^{-9}$	$(6.3 \pm 0.8) \times 10^{-7}$	0.80 ± 0.16

Assuming that H_2O_2 (plus peroxidases) represents the main DCHF sink in intact cells, ROS_i concentrations were then estimated by using a value of the second-order rate constant k_2 established in our laboratory for the reaction of DCHF with H_2O_2 in the presence of horseradish peroxidase ($k_2 = 790 \pm 62$ $M^{-1}s^{-1}$) (see Table I). The mean value of the levels of ROS_i in the four cell lines studied is found to be 0.67 ± 0.16 nM per cell. Remark that the ROSi concentration varies in large scale depending on, cell types, cell cultured conditions and methods used for determining. This value compares favorably to the estimations of the H_2O_2 intracellular steady-state concentrations (1-100 nM) that have been reported in the literature for a few other cell types, such as wild-type *E. coli* and rat liver hepatocytes (Halliwell and Gutteridge, 1999; Giulivi *et al.*, 1999; Cadenas and Davies, 2000).

Overall, our results demonstrate that the non-invasive fluorescence technique used in combination with the DCHF-DA assay is a suitable method for the direct quantitation of intracellular ROS levels in intact drug-sensitive and drug-resistant cancer cells. It is very easy to use, extremely sensitive, and inexpensive. The model presented here is mathematically expressed in Eq. (8) and the parameters intervening in the DCF formation, $k_e = k_1[E]_0$ and $k_2[ROS_i]$, can be quantitatively determined by fitting Eq. (8) to the experimental spectro-fluorometric data. Equation (8) can also be used to estimate ROS_i under other conditions, provided that the concentrations of cells, DCHF-DA and Co^{2+} used in the standardization procedure are maintained.

ACKNOWLEDGEMENTS

One of us (C.L.) is grateful to the Royal Golden Jubilee Ph.D. Program and the French Embassy for their financial support. We also thank Professor Edouard I. Azzam for fruitful correspondence on the physiological concentrations of ROS_i in intact cells.

REFERENCES

Amer J, Goldfarb A and Fibach E (2003). Flow cytometric measurement of reactive oxygen species production by normal and thalassaemic red blood cells. *Eur J Haematol,* 70: 84-90.

Aoyagi K, Akiyama K, Tomida C, Gotoh M, Hirayama A, Takemura K, Ueda A, Nagase S, Koyama A and Narita M (1999). Imaging of hydroperoxides in a rat glomerulus stimulated by puromycin aminonucleoside. *Kidney Int,* 55 (Suppl. 71): S153-S155.

Bass DA, Parce JW, Dechatelet LR, Szejda P, Seeds MC and Thomas M (1983). Flow cytometric studies of oxidative product formation by neutrophils: a graded response to membrane stimulation. *J Immunol*, 130: 1910-1917.

Brandt R and Keston AS (1965). Synthesis of diacetyldichloro-fluorescin: a stable reagent for fluorometric analysis. *Anal Biochem*, 11: 6-9.

Brubacher JL and Bols NC (2001). Chemically de-acetylated 2',7'-dichlorodihydrofluorescein diacetate as a probe of respiratory burst activity in mononuclear phagocytes. *J Immunol Methods*, 251: 81-91.

Burkitt MJ and Wardman P (2001). Cytochrome *c* is a potent catalyst of

dichlorofluorescin oxidation: Implications for the role of reactive oxygen species in apoptosis. Biochem. Biophys. *Res Commun*, 282: 329-333.

Cadenas E and Davies KJA (2000) Mitochondrial free radical generation, oxidative stress, and aging. *Free Rad Biol Med*, 29: 222-230.

Cui S, Reichner JS, Mateo RB and Albina JE (1994). Activated murine macrophages induce apoptosis in tumor cells through nitric oxide-dependent or -independent mechanisms. *Cancer Res*, 54: 2462-2467.

Curtin JF, Donovan M and Cotter TG (2002). Regulation and measurement of oxidative stress in apoptosis. *J Immunol Methods*, 265: 49-72.

Giulivi C, Boveris A and Cadenas E (1999). The steady-state concentrations of oxygen radicals in mitochondria. In: Gilbert, D.L., Colton, C.A. (Eds.), *Reactive Oxygen Species in Biological Systems: An Interdisciplinary Approach* (pp. 77-102), New York: Kluwer Academic/Plenum Publishers.

Grzelak A, Rychlik B and Bartosz G (2001). Light-dependent generation of reactive oxygen species in cell culture media. *Free Rad Biol Med*, 30: 1418-1425.

Gutfreund H (1995). *Kinetics for the Life Sciences: Receptors, Transmitters and Catalysts*. Cambridge University Press, Cambridge.

Halliwell B (2003). Oxidative stress in cell culture: an under-appreciated problem? *FEBS Lett*, 540: 3-6.

Halliwell B and Gutteridge JMC (1999). *Free Radicals in Biology and Medicine*. 3rd edition. Oxford University Press, Oxford.

Homan R and Eisenberg M (1985). A fluorescence quenching technique for the measurement of paramagnetic ion concentrations at the membrane/water interface. Intrinsic and X537A-mediated cobalt fluxes across lipid bilayer membranes. *Biochim Biophys Acta*, 812: 485-492.

Ischiropoulos H, Gow A, Thom SR, Kooy NW, Royall JA and Crow JP (1999). Detection of reactive nitrogen species using 2,7-dichlorodihydro-fluorescein and dihydrorhodamine 123. *Methods Enzymol*, 301 (Part C): 367-373.

Keston AS and Brandt R (1965). The fluorometric analysis of ultramicro quantities of hydrogen peroxide. *Anal Biochem*, 11: 1-5.

LeBel CP, Ischiropoulos H and Bondy SC (1992). Evaluation of the probe 2', 7'-dichlorofluorescin as an indicator of reactive oxygen species formation and oxidative stress. *Chem Res Toxicol*, 5: 227-231.

Loetchutinat C, Kothan S, Jay-Gerin JP and Mankhetkorn S. "Non-invasive spectrofluorometric determination of intracellular reactive oxygen species in drug-sensitive and drug-resistant cells". Poster SD_97P, 29th Congress on Science and Technology, Khon Kaen, Thailand, 20-22 October 2003.

Mankhetkorn S, Dubru F, Hesschenbrouck J, Fiallo M and Garnier-Suillerot A (1996). Relation among the resistance factor, kinetics of uptake, and kinetics of the P-glycoprotein-mediated efflux of doxorubicin, daunorubicin, 8-(*S*)-fluoroidarubicin, and idarubicin in multidrug-resistant K562 cells. *Mol Pharmacol*, 49: 532-539.

Mikkelsen RB and Wardman P (2003). Biological chemistry of reactive oxygen and nitrogen and radiation-induced signal transduction

mechanisms. *Oncogene*, 22: 5734-5754.

Minamiya Y, Abo S, Kitamura M, Izumi K, Kimura Y, Tozawa K and Saito S (1995). Endotoxin-induced hydrogen peroxide production in intact pulmonary circulation of rat. *Am J Respir Crit Care Med*, 152: 348-354.

Morris SJ, Bradley D and Blumenthal R (1985). The use of cobalt ions as a collisional quencher to probe surface charge and stability of fluorescently labeled bilayer vesicles. *Biochim Biophys Acta*, 818: 365-372.

Myhre O, Andersen JM, Aarnes H and Fonnum F (2003). Evaluation of the probes 2', 7'-dichlorofluorescin diacetate, luminol, and lucigenin as indicators of reactive species formation. *Biochem Pharmacol*, 65: 1575-1582.

Ohashi T, Mizutani A, Murakami A, Kojo S, Ishii T and Taketani S (2002). Rapid oxidation of dichlorodihydrofluorescin with heme and hemoproteins: Formation of the fluorescein is independent of the generation of reactive oxygen species. *FEBS Lett*, 511: 21-27.

Reungpatthanaphong P, Dechsupa S, Meesungnoen J, Loetchutinat C and Mankhetkorn S (2003). Rhodamine B as a mitochondrial probe for measurement and monitoring of mitochondrial membrane potential in drug-sensitive and -resistant cells. *J Biochem Biophys Methods*, 57: 1-16.

Rosen GM, Pou S, Ramos CL, Cohen MS and Britigan, BE (1995). Free radicals and phagocytic cells. *FASEB J*, 9: 200-209.

Sheng G, Pu X, Lei L, Tu P and Li C (2002). Tubuloside B from *Cistanche salsa* rescues the PC12 neuronal cells from 1-methyl-4-phenylpyridinium ion-induced apoptosis and oxidative stress. *Planta Med*, 68: 966-970.

Sun AY and Chen Y-M (1998). Oxidative stress and neurodegenerative disorders. *J Biomed Sci*, 5: 401-414.

Tarasiuk J, Foucrier J and Garnier-Suillerot A (1993). Cell cycle dependent uptake and release of anthracycline by drug-resistant and drug-sensitive human leukaemic K562 cells. *Biochem Pharmacol*, 45: 1801-1808.

Ubezio P and Civoli F (1994). Flow cytometric detection of hydrogen peroxide production induced by doxorubicin in cancer cells. *Free Rad Biol Med*, 16: 509-516.

Viidas U, Ahlmen J, Hedner T, Cajdahl K, Larsson A, Pettersson A and Strömbom U (1998). Nitric oxide and blood pressure in normotensive patients on chronic hemodialysis. *Dial Transplant*, 27: 714-724.

Wan CP, Myung E and Lau BHS (1993). An automated micro-fluorometric assay for monitoring oxidative burst activity of phagocytes. *J Immunol Methods*, 159: 131-138.

APPENDIX B

P-glycoprotein-mediated efflux and lysosomal sequestration of drugs confer advantages of K562 MDR sublines to survive prolonged exposure to cytotoxic agents

Submitted to
Indian Journal of Biochemistry and Biophysics

(2006)

P-glycoprotein-mediated efflux and lysosomal sequestration of drugs confer advantages of K562 MDR sublines to survive prolonged exposure to cytotoxic agents

Samarn Dechsupa and Samlee Mankhetkorn*

Laboratory of Physical chemistry, Molecular and Cellular Biology, Department of Radiologic technology, Faculty of Associated Medical Sciences, Chiang Mai University, Chiang Mai 50200 Thailand

Abstract

We sought to clarify the role of Pgp and enhanced lysosomal sequestration of drugs to confer multidrug resistance K562 cells with incremental degree of Pgp-over expression by studying the kinetic uptake of acridine orange and pirarubicin. The mean influx coefficient (k_1) of AO in K562, K562/*adr* and K562/10000 cells was almost the same, about 103 ± 34 $pl.s^{-1}.cell^{-1}$. The mean rate of Pgp-mediated efflux coefficient (k_a) of pirarubicin was easily determined but cannot be determined for AO in K562/*adr* cells. AO exhibited antiproliferative activity and IC_{50} is equal to 447 ± 40 nM, 715 ± 19 nM, and 1,517 ± 274 nM for K562, K562/*adr* and K562/10000 cells, respectively. The cytotoxicity of AO was increased two fold in the co-treatment series using AO and 25 nM monensin. By using the same cell lines and the same method of studies and the different natures of molecular probes, the different predominant cellular defense processes were demonstrated. The MDR phenotype governed by Pgp-mediated efflux can be clearly elucidated using pirarubicin while lysosomal drug sequestration was illustrated using acridine orange. This study clearly showed that both Pgp and lysosomal sequestration of drugs govern the cellular defense mechanisms of MDR cells.

Key words: Multidrug resistance (MDR); P-glycoprotein (Pgp); Acridine orange (AO); Lysosomal drug sequestration; Pirarubicin

*** Corresponding author:** *Tel. 66-53949305; Fax. 66-53946042*
E-mail: samlee@chiangmai.ac.th

INTRODUCTION

Multidrug resistance (MDR) or intrinsic resistance of tumor cells to anticancer agents remains a major cause of treatment failure in cancer therapy. MDR phenomenon is always associated with a decreased intracellular accumulation of anticancer drugs, consequently there is a decline in the therapeutic effect due to an over-expression of MDR protein transporters including Pgp (Gottesman *et al.*, 2002), MRP (Young *et al.*, 2001) and lung resistance related protein (Rybarova *et al.* 2004). MDR is always multifactorial. Many research groups reported that a modification of cellular anticancer drug distribution might be perturbed by an altered pH gradient across different cell compartments. Particularly, acidic organelles such lysosomal sequestration following enhanced exocytosis, which favors a reduced intracellular accumulation of antineoplastic drugs, reducing efficiency, was characterized in various MDR cell types (Miraglia *et al.*, 2005; Altan *et al.*, 1998). Although the

combination of Pgp-mediated flux and the intracellular drug sequestration governed the MDR phenotype was not considered by those researchers. All experiments cited above were performed by using different cell lines or the same cell lines but different degrees of drug resistance and/or with different methods of MDR cell selection. It is of prime importance to demonstrate whether any different observations in MDR cells are caused either by the nature of the cell type or by the different conditions and/or methods of MDR cell selection, yielding variations in the degree of resistance as well as the methods of studies.

We have recently selected MDR cells with Pgp-over expression from the same parental cell line, having increased the degree of resistance by exposing the K562/*adr* to a repetition of fixed adriamycin concentrations (100, 300 and 10000 nM) in a culture medium. We have reported that (i) the *MDR1* mRNA levels and the resistance factor (RF) increased when the concentration of adriamycin used for MDR cell selection increased and (ii) the efficiency of Pgp-mediated efflux is proportional to the RF and the *MDR1* mRNA levels (Meesungnoen *et al.*, 2002).

In this work, we have used the same K562/*adr* (RF=14) and K562/10000 (RF=33) cells as models (Meesungnoen *et al.*, 2002) for investigating the kinetics of uptake, kinetics of active efflux and lysosomal drug sequestration of acridine orange (AO) in comparison with pirarubicin. AO is a lysosomotropic agent, an intrinsic fluorescent, poor substrate of Pgp (compared with pirarubicin) which is frequently used to examine the luminal pH of intracellular acidic organelles (notably lysosome) (Forgac, 1998; Huang *et al.*, 1997; Vercesi and Docampo, 1996; Slapak *et al.*, 1992). The results clearly showed that similar kinetics of uptake of AO was observed in the three cell lines with the mean influx coefficient (k_+) equal to 103 ± 34 $pl.s^{-1}.cell^{-1}$ and the majority of AO was sequestrated in lysosomes but pirarubicin was inconsequential. Similar AO concentration was accumulated in K562 and K562/*adr*, but a significantly lesser degree in K562/10000 cells. The results also clearly demonstrated that both of Pgp-mediated efflux and intracellular drug sequestration conferred multidrug resistance in MDR sublines with highly Pgp-over expression.

MATERIALS AND METHODS

Drugs and chemicals

Adriamycin and pirarubicin (THP) were kindly provided by Professor Arlette Garnier-Suillerot, Laboratoire de Physicochimie Biomoleculaire et Cellulaire, UPRES A 7034 CNRS, UFR Sante Medecine et Biologie Humaine, Bobigny, Universite de Paris Nord. Tetrazolium salt (3–(4, 5–dimethyl –2–thiazolyl)–2,5–diphenyl–2H–tetrazol ium bromide (MTT)) was from Amresco. Monensin was from Sigma.

Adriamycin and pirarubicin stock solutions were prepared in double distilled water just before using. Concentrations were spectro-photometrically determined by diluting stock solutions in water to approximately 10 μM and using ε_{480} = 11,500 $M^{-1}.cm^{-1}$. A stock solution of MTT was prepared by dissolving 5 mg MTT/ml in HEPES-Na^+ buffer and filtering through a 0.22 μm filter and stored in 4 °C.

All experiments were performed using HEPES-Na^+ buffer which consists of 20 mM HEPES buffer plus 132 mM

NaCl, 3.5 mM KCl, 1 mM $CaCl_2$, and 1.5 mM $MgCl_2$, pH 7.25 at 37 °C.

Cell culture and cytotoxicity assay

The human erythromyeloge-nous leukemic, K562 and its Pgp-over expression K562/*adr* (Tarasiuk *et al.*, 1993; Mankhetkorn *et al.*, 1996) were routinely cultured in RPMI 1640 medium supplemented with 10 % fetal calf serum (Gibco Biocult Ltd.). For the assays, a culture was initiated at 5×10^5 cells per ml to have cells in the exponential growth phase; the cells were used 24 hours later, when the culture had grown to approximately 8×10^5 cells per ml. Cell viability was assessed by Trypan blue exclusion. The number of cells was determined by haemocytometer.

The cytotoxicity assay was performed as follow: 5×10^4 cells per ml were incubated in the presence of various THP concentrations. The viability of cells was determined by MTT-reduction. The IC_{50} was determined by plotting the percentage of cell growth inhibition versus the pirarubicin concentration. IC_{50} is the pirarubicin concentration that inhibits cell growth by 50 % when measured at 72 hours. A resistance factor (RF) was defined as the IC_{50} of resistant cells divided by the IC_{50} of the sensitive cells.

Selection of MDR cells

The adriamycin-resistant K562/10000 subline was selected and characterized as previously described by Meesungnoen et *al.* (Meesungnoen et *al.*, 2002). Briefly, K562/*adr* cells were continuously exposed to 10 μM adriamycin in the culture medium for three times with the interval time of 72 hours. The MDR cells were maintained in a fresh medium without doxorubicin for several passages before using.

Theoretical approach for intracellular pH (pH_i) and luminal pH (pH_v) of lysosome determination

AO is a basic molecule (pKa ($-NH^+_3/-NH_2$) = 9.4). In an aqueous solution at a certain pH, it equilibrates in positive charge (DH^+) and neutral (D°) forms as indicated in reaction (1):

$$DH^+ \rightleftharpoons D^o + H^+ \qquad (1)$$

In the presence of cells, only D° passively diffuses through plasma membrane into cytoplasm and intracellular organelles. In a steady state, only the neutral form of AO equilibrates between the extra cellular (D°_e), intracellular (D°_i) and lysosomal (D°_v) compartment; $D^\circ_e = D^\circ_i = D^\circ_v$. In fact the dissociated constant is the same in each compartment, leading the following expression to be written;

$$K_a = \frac{\left(\left[D^0\right]_i\left[H^+\right]_i\right)}{\left[DH^+\right]_i} = \frac{\left(\left[D^0\right]_e\left[H^+\right]_e\right)}{\left[DH^+\right]_e}$$

The pH_i can be determined using the equation (1):

$$pH_e - pH_i = \Delta pH = -\log\frac{\left[DH^+\right]_e}{\left[DH^+\right]_i} \qquad (1)$$

where $[H^+]_i$ and $[H^+]_e$ are the concentration of protons in the intracellular and extra cellular compartments, respectively; $[DH^+]_i$ and $[DH^+]_e$ are the concentrations of positively charged forms of AO in intracellular and extra cellular compartments, respectively.

In pH 7.25, which is approximately the value of the intracellular of most cells, AO is found in 1% of neutral and 99% of positive charged forms. The total concentration of AO is the concentration

of neutral form and charged forms, found in cytoplasm (C_i) and extra cellular (C_e) compartment and can be written as followed:

$$C_i = DH_i^+ + D_i^0 \cong DH_i^+ \quad (2)$$

$$C_e = DH_e^+ + D_e^0 \cong DH_e^+ \quad (3)$$

In the first approximation we replace $[DH^+]_i$ and $[DH^+]_e$ with C_i and C_e, respectively, in equation (1) which becomes

$$\Delta pH = \log \frac{[C_i]}{[C_e]} \quad (4)$$

In our experiments the pH_e was equal to 7.25; then pH_i can be determined:

$$pH_i = 7.25 - \log \frac{[C_i]}{[C_e]} \quad (5)$$

The lysosomal concentration of AO (C_v) can be experimentally determined and the pH_v can be determined in a similar way as pH_i, as written in equation (6):

$$pH_v = pH_i - \log \frac{[C_v]}{[C_i]} \quad (6)$$

Subcellular distribution of acridine orange

In order to determine the kinetics of uptake, the kinetics of Pgp-mediated efflux, the overall cellular AO concentration and the lysosomal AO concentration, a continuous dialysis device was coupled with the spectrofluorometer (Perkin Elmer LS 50 B) and was applied in the experiments. The experiments were conducted in a 1-cm optical quartz cuvette containing 3.5 ml of buffer solution with 0.2 μm pore diameter membrane dialysis compartment (a container of cells) placed on the top, and was continuously stirred at 37 °C. The excitation beam was passed through the bottom part of the cuvette, which means only AO in supernatant was excited. The fluorescence intensity of AO at 527 nm (excited at 491 nm) was measured as a function of time. After an addition of AO to the system, we observed that the fluorescence intensity decreased, due to some quantity of AO being adsorbed onto the surface of the dialysis compartment. The steady state was reached in 30 minutes and the fluorescence intensity became F_T. The fluorescence intensity F_T was proportional to the AO concentration added, up to 5 μM.

The C_T corresponds to the quantities of AO available for the experiment and can be determined as follow:

$$C_T = C_T^0 \times \left(\frac{F_0}{F_T} \right) \quad (7)$$

where C^0_T and F_0 is the known final AO concentration added into a cuvette and its corresponding fluorescence intensity, respectively.

It was verified that the AO fluorescence spectral shape and intensity did not change in the supernatant of cells. Cells (10^6cells/ml) were introduced into the dialysis compartment; a decrease in AO fluorescence intensity was due to the extra cellular drug, which passes through the dialysis membrane to reach and be incorporated by cells. A new steady state was attained at 60 minutes where AO fluorescence intensity was identified as F_c, after which 3 μM monensin was added for eliminating any intracellular pH gradient (ΔpH) formation resulting to increase in AO fluorescence intensity to be F_{mon}. Thereafter 0.02% (V/V) saponin was successively added, resulting in total permeability of the plasma membrane leading the system to reach the equilibrium state. In steady state, the free

extra cellular (C_e) and lysosomal (C_v) AO concentration can be calculated from equation (8) and (9):

$$C_e = C_T \times \left(\frac{F_c}{F_T} \right) \quad (8)$$

$$C_v = C_T \times \left\{ \frac{(F_{mon} - F_c)}{F_T} \right\} \quad (9)$$

where F_{mon} is AO fluorescence intensity at a steady state after the addition of 3 μM monensin.

In the presence of 3 μM monensin, any intracellular pH gradient (ΔpH) formation in particular lysosomes was eliminated. A new steady state was reached where AO equilibrates between extra cellular and cytoplasm compartment.

The extra cellular (C_E) and cytoplasm (C_I) AO concentration can be determined using equation (10) and (11):

$$C_I = C_T \times \left\{ \frac{(F_T - F_{mon})}{F_T} \right\} \quad (10)$$

$$C_E = C_T \times \left(\frac{F_{mon}}{F_T} \right) \quad (11)$$

The intracellular AO concentration (C_i) at steady state after addition of cells can be determined:

$$C_i = C_e \times \left(\frac{C_I}{C_E} \right) \quad (12)$$

The initial rate of uptake $(V_+)_{t=0}$ (passive influx) was determined from the equation $V_+ = \left| \left(\frac{dF}{dt} \right)_{t=cell} \right| \cdot \left(\frac{C_T}{F_T} \right)$, where $\left| \left(\frac{dF}{dt} \right)_{t=cell} \right|$ is the slope (in absolute value) of tangent to the curve F = f(t). The rate of Pgp-mediated efflux $(V_a)_s$ of acridine orange was determined as followed (Mankhetkorn *et al.*, 1996):

$$(V_a)_S = k_+ \times n \times (C_e - C_i) \quad (13)$$

Cellular uptake and the Pgp-mediated efflux of pirarubicin

The rationale and validation of the experimental setup for measuring the kinetics of uptake and Pgp-mediated efflux of pirarubicin in cells have been largely described (Meesungnoen *et al.*, 2002; Tarasiuk *et al.*, 1993; Mankhetkorn *et al.*, 1996). Briefly, in a typical experiment, conducted in a 1-cm quartz cuvette containing 2 mL of HEPES–Na^+ buffer, 2×10^6 cells were incubated for 30 minutes in the presence of 10 mM of sodium azide and in the absence of glucose, under continuous stirring at pH 7.25 and 37°C. The concentration of pirarubicin added to the cell suspension was varied from 0.5 to 10 μM. The fluorescence intensity of pirarubicin at 590 nm (excitation at 480 nm) was followed as a function of time (model LS 50 B spectrofluorometer, PerkinElmer). The drug influx was measured by the decrease of the fluorescence intensity that occurred during incubation with cells due to the quenching of the fluorescence after pirarubicin intercalates between the base pairs of DNA in nuclei or accumulates into acidic intracellular organelles. This present methodology allowed us to measure accurately the free cytosolic concentration of pirarubicin in a steady state (C_i), its initial rate of uptake (V_i^+), and the rate of Pgp-mediated efflux (V_a). At the end of the experiment, intactness of cells was confirmed by trypan blue exclusion.

Fluorescence micrograph and flow cytofluorometric assay

Human primary culture enriched in myoblastic cells were cultured in RPMI 1640 medium supplemented with 20% fetal bovine serum (Gibco Biocult Ltd.) and 1% penicillin-streptomycin. For the assays, a culture was initiated at 10^5 cells per ml and allowed to grow to approximately 70% confluence. The culture medium was removed and rinsed once adding HEPES-Na^+ buffer pH 7.25. AO (1 μM) was added into the cells and it was allowed to further incubate at 37°C for 30 minutes prior to placement on the sample holder of inverted fluorescence microscope (Nikon model TE-2000E) using a filter box model B-2E/C coupled with Nikon, digital camera model DXM 1200F. The ratio of red to green fluorescence was analyzed using flow a cytometer (Coulter Epics XL-MCL).

RESULTS

Cytotoxic effects of acridine orange and THP

Figure 1 illustrates the efficacy of AO and pirarubicin alone to inhibit cancer growth. For drug-sensitive K562 cells, pirarubicin potently exhibited anticancer activities (IC_{50} = 12.5 ± 2.5 nM) and was 36-fold more effective than AO. Both pirarubicin and AO were less cytotoxic against drug-resistant sublines; the IC_{50} of the pirarubicin and AO are equal to 175 ± 35 nM and 715 ± 19 nM for K562/*adr* and 410 ± 85 nM and 1,517 ± 274 nM for K562/10000 cells, respectively. Figure 1 also illustrates the efficacy of co-treatment using AO or pirarubicin with 25 nM monensin. It should be noted that 25 nM monensin did not affect the viability of the cells used in these experiments. The co-treatment results clearly showed that in the presence of 25 nM monensin, the IC_{50} of AO significantly decreased in both drug-sensitive and drug-resistant sublines (Figure 1a) while slightly affected in the series of experiments using pirarubicin (Figure 1b) in K562/10000 and no effect in K562 and K562/*adr* cells.

Cellular distribution of AO

Human myoblastic cells were used to demonstrate cellular distribution of AO because of its large space of cytoplasm and nucleus localized at the central of cell. The cellular distribution of AO was clearly shown in Figure 2. The bright green fluorescence of AO corresponded to an amount of AO binding to the cytoskeleton demonstrating the cytoplasm. The dense circles with orange fluorescence were found outside the nucleus and this orange fluorescence disappeared in the presence of 3 μM monensin. The orange fluorescence represents lysosomes. The ratio of red to green fluorescence representing the amounts of AO localized in lysosomes and cytoplasm was analyzed using flow cytometer.

Determination of the lysosomal concentration (C_v) and mean influx coefficient (k_+) of AO

In order to quantitatively measurement the lysosomal concentration (C_v) of AO, a system containing a continuous dialysis device coupled with the spectrofluorometer was applied to follow the AO fluorescence intensity in solution at the bottom part of the cuvette where it represented the extra cellular AO concentration.

Figure 3 demonstrates typical kinetics of uptake of AO by K562 cells. The AO fluorescence intensity decayed as a function of time to reach a steady state at 100 minutes. In order to verify that cellular incorporation of AO, at the steady state cells were taken and injected into flow cytometer to analyse the ratio of red to green fluorescence. The concentration of lysosomal AO concentration (C_v) was evaluated by successive addition of incremental monensin concentration into cells yielding an increase in fluorescence intensity of AO which corresponded to the amount of AO released from lysosomes to the extra cellular compartment. ΔFluorescence intensity, the difference of AO fluorescence intensity before and after addition of monensin, corresponding to the C_v as a function of concentration of monensin added was indicated in the inset of Figure 3. The maximal lysosomal AO concentration was determined when 3 μM monensin was added.

The representative kinetics of AO uptake in K562, K562/*adr* and K562/10000 were shown in Figure 4a. The initial rate of uptake (V_i^+) was determined in all cell lines used and found to be proportional to C_T added as indicated in Figure 4b. This signified that in the concentration range used, AO in neutral form passively diffused across plasma membrane into cells. The mean influx coefficient of AO (k_+) was obtained by linear least-square fit of data of Figure 4b of the three cell lines and was equal to 103 ± 34 $pl.s^{-1}.cell^{-1}$. The C_v was identical and reached a pseudo-plateau when the concentration of AO added was above 1.75 μM in K562 cells and K562/*adr* cell. However, it was found that very low quantities of AO accumulated in K562/10000 cells (Figure 4c).

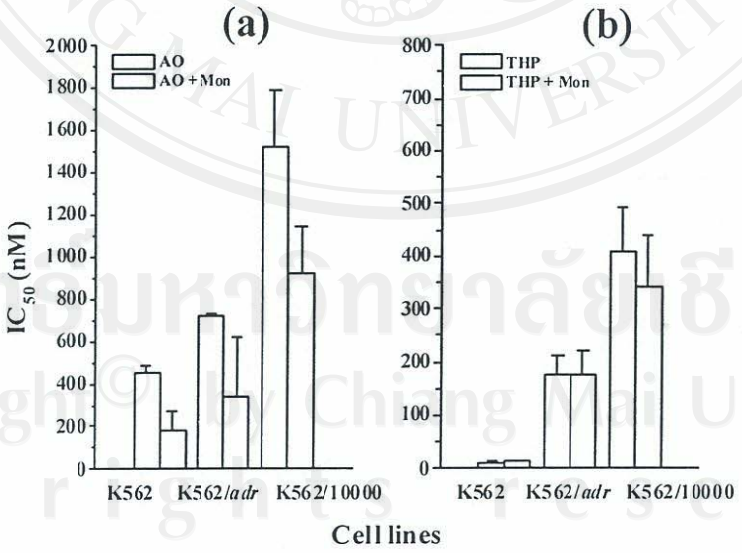

Figure 1. Drug response pattern of MDR cell lines. IC_{50} of (a) acridine orange alone (☐) and in combination with 25 nM monensin (☐), and (b) pirarubicin alone (☐) and in combination with 25 nM monensin (☐).

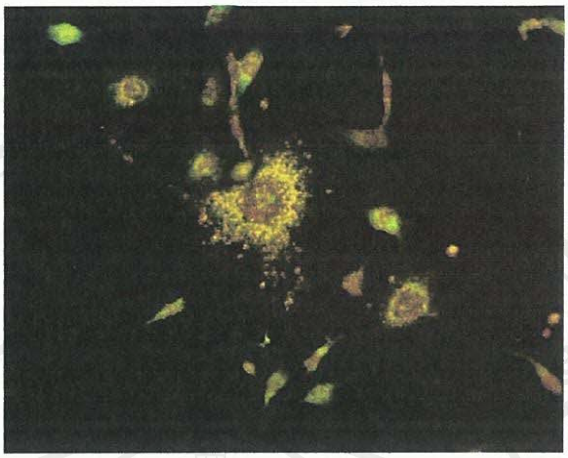

Figure 2. Fluorescence micrograph of human myoblastic cells showing lysosomes (orange or red fluorescence in circles) and cytoplasm (green fluorescence). Cells of density approximately 70% confluence were in a culture flask; the culture medium was removed and rinsed once using HEPES-Na^+ buffer pH 7.25. AO (1 μM) was added into the cells and allowed to further incubation at 37℃ for 1 hour prior to placement on the sample holder of inverted fluorescence microscope.

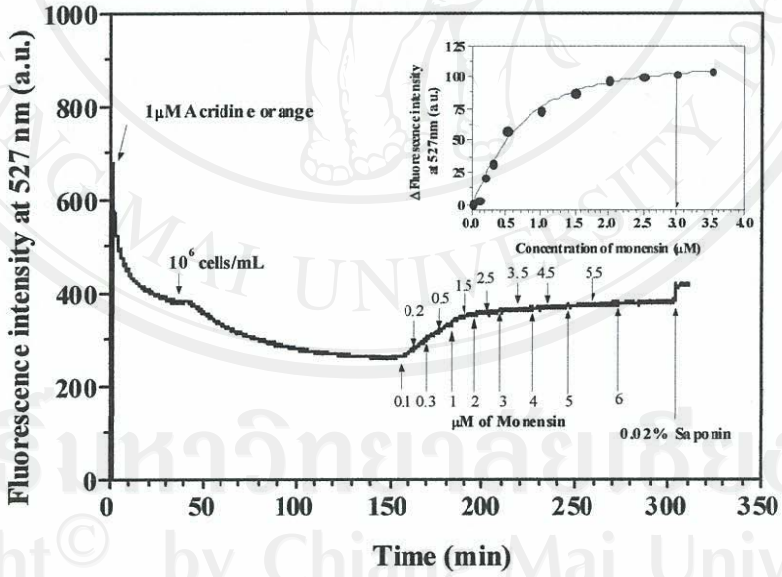

Figure 3. Quantitative measurement of lysosomal acridine orange (AO) concentration. The fluorescence intensity at 527 nm (excited at 491 nm) was registered as a function of time. AO (1 μM) was added into the cuvette containing 3.5 mL of HEPES-Na^+ buffer at 37 °C and vigorously stirred. At steady state, $3.5x10^6$ cells were added, yielding a progressive decrease in fluorescence intensity then reached a new steady state, and after that indicated monensin concentration was added at the same interval of time.

Inset of Figure 3. ΔFluorescence intensity at 527 nm as a function of concentration of monensin added.

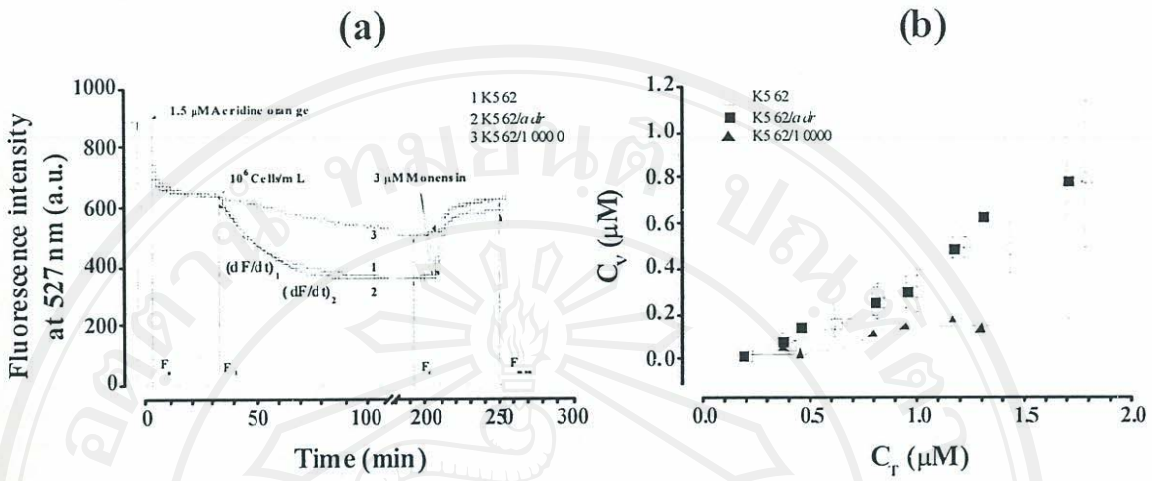

Figure 4. (a) A typical acridine orange uptake by three cell lines: (1) K562, (2) K562/*adr* and (3) K562/10000 cells, (b) initial rate of uptake and (c) intralysosmal concentration (C_v) of AO in (□) K562, (■) K562/*adr* and (▲) K562/10000 cell lines as a function of total concentration (C_T) of AO added. Cells were incubated in 1-cm quartz cuvette containing 3.5 ml HEPES-Na^+ buffer at 37 °C and vigorously stirred. After the addition of AO, the fluorescence intensity detected at 527 nm (excitation wavelength 491 nm) was F_0, and decreased progressively until the system reached a steady state (F_T). Then $3.5x10^6$ cells were added yielding a progressive decrease in fluorescence intensity at 527 nm which corresponded to amounts of AO passively diffused through plasma membrane. After the system reached a new steady state (F_c), the pH gradient was eliminated by 3 μM monensin resulting in an increased in fluorescence intensity, after which and then a new steady state was reached and characterized by the fluorescence intensity value F_{mon}. This corresponded to liberation of the lysosomal AO (C_v) to cytoplasm and extra cellular compartments. The lysosomal (C_v) and the initial rate of uptake (v_i^+) of AO can be determined using the following equation $C_v = C_T \times \left\{ \frac{(F_{mon} - F_c)}{F_T} \right\}$ and $V_i^+ = \left(\frac{dF}{dt} \right)_c$, repectively.

P-glycoprotein-mediated efflux of pirarubicin and AO

The MDR phenotype of K562/*adr* and K562/10000 was characterized and previously reported by our group (Meesungnoen *et al.*, 2002). In the range of total concentration of pirarubicin used, the accumulation in compartments other than the nucleus was negligible. Figure 5a showed that K562/*adr* cells contained functional Pgp (k_a = 2.6 ± 0.9 pl.s^{-1}.cell^{-1}) which extruded piraribicin out of cells about two fold lesser than K562/10000 cells (4.7 ± 1.0 pl.s^{-1}.cell^{-1}). It should be noted that the kinetics of Pgp-mediated efflux of AO determined from K562/*adr* cells was very low and cannot be determined by using this method. However, the initial rate of active efflux of AO was easily measured from K562/10000 as indicated in Figure 5b. In this series of experiments the saturation of initial rate of active efflux was not obtained. The mean rate constant of active efflux (k_{ae}) of AO was equal to 1,930 ± 300 pl.s^{-1}.cell^{-1}.

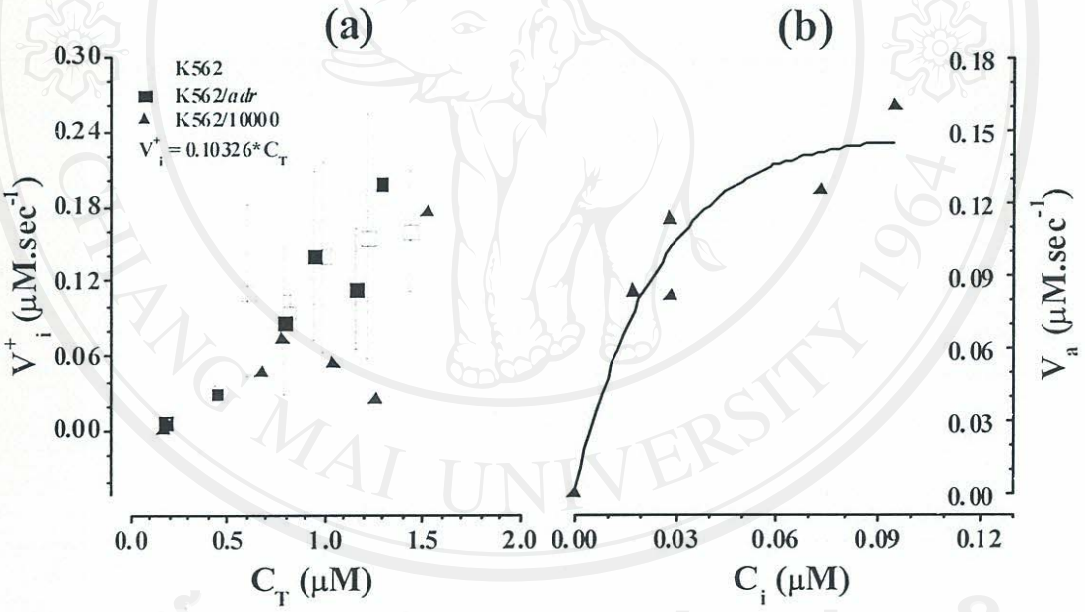

Figure 5. The Pgp-mediated efflux of (a) pirarubicin and (b) AO determined from (■) K562/*adr* and (▲) K562/10000 cells plotted as a function of free cytosolic concentration (C_i) of pirarubicin or AO added. The results were obtained from the series of experiments with the same conditions as Figure 4. The transport of THP is best described by Hill's equation of enzyme kinetics; $V_a = \frac{V_{max}.C_i^{nH}}{K_m^{nH} + C_i^{nH}}$ where K_m was 1.05 ± 0.01 μM and V_{max} was 2.6 ± 0.9 nM.s^{-1}for K562/*adr* and 4.7 ± 1.0 nM.s^{-1}, respectively. Hill's coefficient (*nH*) was near to 1.95. The line represents the mean value from the triplicate data.

DISCUSSION

The results clearly showed that AO was exclusively accumulated in acidic organelles particularly lysosomes, whereas the nuclear compartment was reported as its potential intracellular target (Kusuzaki *et al.*, 2000; Dobrucki and Darzynkiewicz, 2001; Grunwald, 1993). In fact that the efficacy of AO was significantly improved when cells were incubated in the presence of 25 nM monensin. This resulted in an elimination of intracellular ΔpH formation and consequently the releasing of AO from lysosomes to the cytosolic compartment. These were followed by an increase in free cytosolic and nuclear compartments of AO concentrations thus increased in efficacy. However, after an elimination of pH gradient formation, MDR cells were still more resistant to AO than their corresponding parental K562 cells indicating the Pgp-mediated efflux should take into account predominant mechanism of the MDR phenotype. Contrary to pirarubicin, an intercalator drug that was preferable accumulated on nuclear compartment, its potential intracellular target with the k_+ equal to 3.4 ± 0.3 $pl.s^{-1}.cell^{-1}$. Although the function of lysosomes was inhibited in the presence of 25 nM monensin, K562/*adr* cells did not exhibit any additional sensitivity to pirarubicin, and only slightly did in K562/10000 cells. This signified that an accumulation of pirarubicin at lysosomes did not contribute to drug resistance in K562/*adr* cells and seemed to take role when MDR cells became higher resistance such as K562/10000 cells.

AO was passively diffused through the plasma membrane of K562, K562/*adr* and K562/10000 cells with the same k_+ that was equal to 103 ± 34 $pl.s^{-1}.cell^{-1}$, while the mean influx coefficient, k_+ of pirarubicin was equal to 3.4 ± 0.3 $pl.s^{-1}.cell^{-1}$. There was strong evidence that Pgp played a predominant role to convey drug resistance, even in highly resistance phenotypes since the k_a was determined, equal to 2.6 ± 0.9 $pl.s^{-1}.cell^{-1}$ and 4.7 ± 1.0 $pl.s^{-1}.cell^{-1}$ for K562/*adr* and K562/10000 cells, respectively. As for AO, the k_a was not able to be measured from K562/*adr* cells and its kinetic of uptake was similar to that of K562 cells. This should be interpreted as AO being a poor substrate of Pgp and that the k_+ is very fast compared with the k_a. In these conditions, Pgp should be saturated and the activity of Pgp per times turn over cannot maintain the gradient between extra cellular and intracellular AO concentration. It should be noted that K562/10000 cells contained only about twofold more functional Pgp than K562/*adr* cells but the mean rate of active efflux was 1,930 ± 300 $pl.s^{-1}.cell^{-1}$. It was not possible that this active efflux could be generated by Pgp, but other mechanisms that can convey numerous molecules of AO from cytoplasm to the exterior of cells per turn was probably a characteristic of an enhanced exocytosis of lysosomal sequestrated AO. This was consistent in the observation that the C_v was very low in K562/10000 cells.

The accumulation of AO in lysosomes and cytoplasm can also give information about physico-chemical properties of microenvironments, especially the local pH. Under these experimental conditions, the concentrations of AO in each compartment were calculated in molar units (global concentration) allowed us to determine pH_i and pH_v (see materials and methods) as indicated in Figure 6. The pH_i for all cell lines used in these experiments was about 7.25 (Figure 6a). The pH_v as a function of C_v is indicated

in Figure 6b. In K562 and K562/*adr* cells, the pH_v increased with C_v then reached a plateau when C_v was equal to 0.5 μM where pH_v about 7.2 closely to pH_i. These results suggested that either the H^+-ATPase pump may be saturated or the maximum volume of these organelles could be attained when there was enough concentration of the basic molecule inside. The initial pH_v (without AO inside), was extrapolated from the function of $pH_V = \int(C_V)$ using a non-linear plot (Boltzman's curve) for K562 and K562/*adr* cell lines and was equal to 6.30. Similar results were obtained in K562/10000 cells but no saturation of pH_v was obtained because of too low C_v; the data were linearly least-square fitted and the initial pH_v value was about 5.70. These agree with the reports from other research groups both acidified of pH_v and alkalinized of pH_i of MDR cells compared with its corresponding drug-sensitive cells. For example, it was found that the ΔpH was 1.2 and 0.3 unit in multidrug resistant (pH_i = 7.1 ± .025) and sensitive MCF-7 cells (pH_i = 6.8 ± .025), respectively (Altan *et al.*, 1998; Dell'Antone and Piergallini, 1997; Ferderick *et al.*, 1990; Schindler *et al.*, 1996; Belhoussine *et al.*, 1999; Roepe *et al.*, 1993). In addition, Altan *et al.* found an acidification of lysosome in drug-resistant cells (Altan *et al.*, 1998).

The application of AO, an intrinsic fluorescent weak base molecule as molecular probe allowed monitoring of spontaneous changes in pH_i during AO incorporation into cells (Figure 6a). The results suggested that the uptake of AO stimulated an acidification of pH_i in MDR cells with high degree of resistance. It is very important to note that AO did not induce any pH_i change in K562/*adr* cell. We recently reported that in K562/10000 cells, the K^+/H^+ antiporter exchanger could be activated by THP transport, leading to an acidification of pH_i (Meesungnoen *et al.*, 2002). In fact that maintenance of pH_i within a narrow physiological range is vital to normal cell function. Nevertheless, the intracellular free H^+ can vary in response to different stimuli. Increasing evidence indicates that intracellular protons can serve as a second messenger in regulating multiple cellular functions (Filosa *et al.*, 2002; Berger *et al.*, 1998).

The results clearly demonstrated that by using the same cell lines and the same method of studies, but the different natures of molecular probes such as AO and pirarubicin, the different predominant cellular defense processes were elucidated. In fact the role of Pgp-mediated efflux of cytotoxic drug out of the cell conferring lower available intracellular concentration thereby lower efficiency can be clearly demonstrated using pirarubicin. The lysosomal drug sequestration was also a major cause of lowering available intracellular concentration of the drug which provided the advantages for the MDR cells, particularly K562/10000 cells, to survive prolonged exposure to cytotoxic agents and thus to contribute to chemotherapeutic resistance. The predominant mechanism of MDR phenomenon is totally depended on the nature of the molecules.

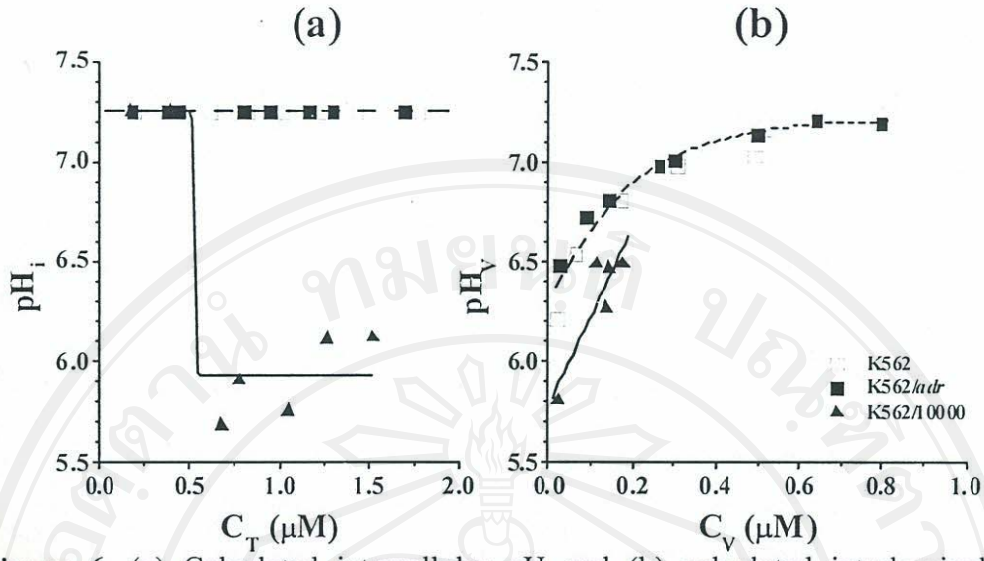

Figure 6. (a) Calculated intracellular pH and (b) calculated intraluminal pH of lysosomes of (□) K562, (■) K562/*adr* and (▲) K562/10000 cell lines as a function of concentration of AO.

ACKNOWLEDGEMENTS

This study was partly supported by the Royal Thai Government and the Royal Golden Jubilee program (RGJ). S.D. thanks the Royal Golden Jubilee Ph.D. program for financial support.

REFERENCES

Altan N, Chen Y, Schindler M and Simon SM (1998). Defective acidification in human breast tumor cells and implications for chemotherapy. *J Exp Med*, 187: 1583-1598.

Belhoussine R, Morjani H, Sharonov S, Ploton D and Manfait M (1999). Characterization of intracellular pH gradients in human multidrug-resistant tumor cells by means of scanning microspectrofluorometry and dual-emission-ratio probes. *Int J Cancer*, 81: 81-89.

Berger MG, Vandier C, Bonnet P, Jackson WF and Rusch NJ (1998). Intracellular acidosis differentially regulates KV channels in coronary and pulmonary vascular muscle. *Am J Physiol*, 275: H1351-1359.

Dell'Antone P and Piergallini L (1997). The antineoplastic drug lonidamine interfieres with the acidification mechanism of cell organelles. *Biochim. Biophys Acta*, 1358: 46-52.

Dobrucki J and Darzynkiewicz Z (2001). Chromatin condensation and sensitivity of DNA in situ to denaturation during cell cycle and apoptosis; a confocal microscopy study. *Micron*, 32: 645-652.

Ferderick CA, Williams LD, Ughetto G, van der Marel GA, van Boom JH, Rich A and Wang AHJ (1990). Structural comparison of anticancer drug-DNA complexes: adriamycin and daunorubicin. *Biochem J*, 29: 2538-2549.

Filosa JA, Dean JB and Putnam RW (2002). Role of intracellular and extra cellular pH in the chemosensitive response of rat locus coeruleus neurones. *J Physiol*, 541: 493-509.

Forgac M (1998). Structure, function and regulation of the vacuolar (H+)-ATPases. *FEBS Lett*, 440: 258-263.

Gottesman MM, Fojo T and Bates SE (2002). Multidrug resistancein cancer: role of ATP-dependent transporters. *Nat Rev Cancer*, 2: 48-58.

Grunwald D (1993) Flow cytometry and RNA studies. *Biol Cell*, 78: 27-30.

Huang SS, Koh HA and Huang JS (1997). Suramin enters and accumulates in low pH intracellular compartments of v-sis-transformed NIH 3T3 cells. *FEBS Lett*, 416: 297-301.

Kusuzaki K, Minami G, Takeshita H, Murata H, Hashiguchi S, Nozaki T, Ashihara T and Hirasawa Y (2000). Photodynamic inactivation with acridine orange on a multidrug-resistant mouse osteosarcoma cell line. *Jpn J Cancer Res*, 91: p. 439-445.

Mankhetkorn S, Dubru F, Hesschenbrouck J, Fiallo M and Garnier-Suillerot A (1996) Relation among the resistance factor, kinetics of uptake, and kinetics of the P-glycoprotein-mediated efflux of doxorubicin, daunorubicin, 8-(S)-fluoroidaru-bicin, and idarubicin in multidrug-resistant K562 cells. *Mol Pharmacol*, 49: 532-539.

Meesungnoen J, Jay-Gerin JP and Mankhetkorn S (2002). Relation between MDR1 mRNA levels, resistance factor, and the efficiency of P-glycoprotein-mediated efflux of pirarubicin in multidrug-resistant K562 sublines. *Can J Physiol Pharmacol*, 80: 1054-1063.

Miraglia E, Viarisio D, Riganti C, Costamagna C, Ghigo D and Bosia A (2005). Na(+)/H(+) exchanger activity is increased in doxorubicin-resistant human colon cancer cells and its modulation modifies the sensitivity of the cells to doxorubicin. *Int J Cancer*, 115: 924-929.

Roepe PD, Wei LY, Cruz J and Carlson D (1993). Lower electrical membrane potential and altered pHi homeostasis in multidrug-resistant (MDR) cells: further characterization of a series of MDR cell lines expressing different levels of P-glycoprotein. *Biochem J*, 32: 11042-11056.

Rybarova S, Hajdukova M, Hodorova I, Kocisova M, Boor A, Brabencova E, Kasan P, Biros E, Mojzis J and Mirossay L (2004). Expression of the multidrug resistance-associated protein 1 (MRP1) and the lung resistance-related protein (LRP) in human lung cancer. *Neoplasma*, 51: 169-174.

Slapak CA, Lecerf JM, Daniel JC and Levy SB (1992). Energy-dependent accumulation of daunorubicin into subcellular compartments of human leukemia cells and cytoplasts. *J Biol Chem*, 267: 10638-10644.

Schindler M, Grabski S, Hoff E and Simon SM (1996) Defective pH regulation of acidic compartments in human breast cancer cells (MCF-7) is normalized in adriamycin-resistant cells (MCF-7adr). *Biochem J*, 35: 2811-2817.

Tarasiuk J, Foucrier J and Garnier-Suillerot A (1993). Cell cycle dependent uptake and release of anthracycline by drug-resistant and drug-sensitive human leukaemic K562 cells. *Biochem Pharmacol*, 45: 1801-1808.

Vercesi AE and Docampo R (1996). Sodium-proton exchange stimu-lates Ca^{2+} release from acido-calcisomes of trypanosoma brucei. *Biochem J*, 315: 265-270.

Young LC, Campling BG, Cole SP, Deeley RG and Gerlach JH (2001). Multidrug resistance proteins MRP3, MRP1, and MRP2 in lung cancer: Correlation of protein levels with drug response and messenger RNA levels. *Clin Cancer Res*, 7: 1798-1804.

CURRICULUM VITAE

NAME: **Mr. Samarn Dechsupa**

(New) Mr. Nathupakorn Dechsupa

DATE OF BIRTH: **12 October 1975**

PLACE OF BIRTH: **Prachin Buri, Thailand**

INSTITUTE ATTENED

YEAR	Description of qualification	Place obtained
2006	Doctor of Philosophy (Biomedical Science)	Chiang Mai University, Chiang Mai, Thailand
2001	Master of Science (Biological Sciences)	Burapha University, Chonburi, Thailand
1998	Bachelor of Science (Physics)	Burapha University, ChonburiThailand
1994	Certificate of Matayomsuksa 6	Prachin Rasadorn Umrung School, Prachin buri, Thailand
1991	Certificate of Matayomsuksa 3	Tha Kasaem Pitthaya School, Sakaeo, Thailand
1988	Certificate of Prathomsuksa 6	Ban Tha Kasaem School, Sakaeo, Thailand

RESEARCH GRANT

Year	Researcher Assistant of the Royal Golden Jubilee Ph.D. program
2001	RGJ#PHD0101/44